

Determination of 6-mercaptopurine in the presence of uric acid using modified multiwall carbon nanotubes-TiO₂ as a voltammetric sensor

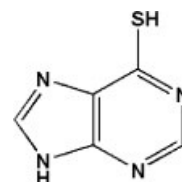
Ali A. Ensafi* and H. Karimi-Maleh

In this work, a multiwall carbon nanotubes modified electrode (prepared by incorporating TiO₂ nanoparticles with *p*-aminophenol as a mediator) was used as voltammetric sensor for the determination of 6-mercaptopurine (6-MP) in the presence of uric acid (UA). The voltammograms of 6-MP and UA in a mixture can be separated from each other by differential pulse voltammetry with a potential difference of 380 mV at a scan rate of 10 mV s⁻¹. These conditions are sufficient to allow for the determination of 6-MP and UA both individually and simultaneously. The electrocatalytic currents increase linearly with 6-MP concentration in the ranges of 0.09–350 μmol L⁻¹ (two linear segments with different slopes). The detection limit for 6-MP was 0.065 μmol L⁻¹. The RSD% for 1.0 and 15.0 μmol L⁻¹ 6-MP were 0.7%, and 1.2%, respectively. The kinetic parameters of the system were determined using electrochemical approaches. The method was successfully applied for the determination of 6-MP in drug sample, and 6-MP plus UA in urine samples. Copyright © 2011 John Wiley & Sons, Ltd.

Keywords: 6-Mercaptopurine and uric acid determination; electrocatalytic method; *p*-aminophenol; voltammetry.

Introduction

Mercaptopurine (also called 6-mercaptopurine, 6-MP), Scheme 1, is an immunosuppressive drug. It is a thiopurine^[1] and used to treat leukaemia. This drug is traditionally not recommended during pregnancy but this issue has been debated and current evidence indicates that pregnant women on the drug show no increase in foetal abnormalities. However, women receiving mercaptopurine during the first trimester of pregnancy have an increased incidence of abortion. Therefore, the drug has the potential to be cancer-causing in humans. Various methods including high performance liquid chromatography (HPLC),^[2–6] capillary electrophoresis,^[7–10] electrochemical methods,^[11,12] fluorescence,^[13,14] and spectrophotometric methods^[15] have been used for the detection of 6-MP in plasma. Recently, in order to obtain an effective separation and sensitive detection, some coupled methods such as capillary electrophoresis with laser-induced fluorescence,^[16] liquid chromatography with electrochemical detection,^[17] and liquid chromatography with microdialysis^[18] have been used for monitoring 6-MP. 6-MP-coated gold nanoparticles have more recently been prepared with excellent stability and the enhanced spectroscopic signal has also been used for detecting 6-MP.^[19–21] However, there still remain certain limitations in spectrofluorimetric and chromatographic methods that include selecting a suitable column or mobile phase, finding a suitable reactant for the post-column reaction (in order to increase sensitivity) in liquid chromatography, and facing many interfering substances in spectrofluorimetric methods. Most of the methods reported suffer from disadvantages such as complicated procedure, long response time, requirement of expensive instruments, and low detection capability.



Scheme 1. The structure of 6-MP.

Uric acid (2,6,8-trihydroxypurine, UA), the end metabolic product of purine through the liver, is present in blood and urine. Monitoring UA in the blood or urine is important because it can be used as a powerful indicator for an early warning sign of kidney diseases. There are some electrochemical methods for the determination of UA.^[22–27] On the other hand, for many of them, 6-MP acts as interference. However, for patients on 6-MP, UA and 6-MP concentrations should be checked for high levels of UA. If positive, then the patient needs to be hydrated, or his/her urine alkalized; allopurinol can also be used in such cases as a helping drug.^[28] Thus, in patients undergoing treatment with 6-MP, UA is excreted in more quantity in comparison to controls. Therefore, simultaneous determination of 6-MP and UA is vital.

Carbon nanotubes (CNTs) continue to receive considerable attention in electrochemistry.^[29–36] CNTs have been the subject of numerous investigations in chemical, physical, and materials

* Correspondence to: Ali A. Ensafi, Department of Chemistry, Isfahan University of Technology, Isfahan 84156–83111, Iran. E-mail: Ensafi@cc.iut.ac.ir

Department of Chemistry, Isfahan University of Technology, Isfahan 84156–83111, Iran

Table 1. Comparison of the efficiency of some methods in the determination of 6-MP

Methods	Limit of detection ($\mu\text{mol L}^{-1}$)	Linear dynamic range ($\mu\text{mol L}^{-1}$)	Reference
DPV ^a	16 000	16 000–67 500	11
Fluorescence	0.02	0.066–40	13
HPLC ^b	0.006	0.013–0.4	6
Fluorescence	0.0004	0.06–0.3	8
DPV	0.08	0.2–50	12
DPV	0.065	0.09–350	This work

^a Differential pulse voltammetry.^b High performance liquid chromatography.

areas due to their novel structural, mechanical, electronic, and chemical properties.^[37,38] CNT modified electrodes have been reported to give super-performance in the study of a number of biological species, including levodopa,^[39] cytochrome c,^[40] UA,^[41] epinephrine,^[42] and glutathione.^[43] Few publications are available regarding electrochemical determination of just 6-MP in real samples using chemically modified electrodes.^[11,18] In all of the reported methods, UA acts as an interfering compound, hence needs separation before analysis, because it affects the selectivity. As yet, based on our knowledge, no paper has been reported on the simultaneous determination of 6-MP pulse UA using electrochemical methods. Comparisons of the results obtained from different methods are given in Table 1.

In this paper, we have used voltammetric and electrochemical impedance spectroscopic techniques to demonstrate the electrochemical behaviour of 6-MP on multiwall carbon nanotubes-TiO₂ paste electrode modified with *p*-aminophenol. The proposed sensor is highly selective and sensitive for the determination of 6-MP in the presence of UA. The detection limit, linear dynamic range, and sensitivity to 6-MP with the *p*-aminophenol modified carbon nanotubes paste electrode (*p*-APMCNTPE) from this method are comparable to, and even better than, those from recently developed which use voltammetric methods. Although the oxidation peak of UA overlapped with that of 6-MP with the other electrodes, this electrode was able to differentiate the substances and it is, therefore, possible to measure both simultaneously. The proposed method suffers from lower limit of detection and higher selectivity and it could be use for simultaneous determination of 6-MP and UA.

Experimental

Chemicals

All chemicals used were of analytical reagent grade purchased from Merck (Darmstadt, Germany) unless otherwise stated. Doubly distilled water was used throughout. *p*-Aminophenol was used from Fluka and 6-MP from Merck (Darmstadt, Germany).

Universal buffer (boric acid, phosphoric acid, acetic acid plus sodium hydroxide, 0.10 mol L⁻¹) solutions with different pH values were used.

High viscosity paraffin ($d = 0.88 \text{ kg L}^{-1}$), graphite powder (particle size <50 μm) and carbon nanotubes (>9% MWCNT basis, $d \times l = (110-70 \text{ nm}) \times (5-9 \mu\text{m})$) from Fluka (Buchs, Switzerland) were used as a substrate for preparation of the carbon paste electrode as a working electrode (WE).

Apparatus

Cyclic voltammetry (CV) and differential pulse voltammetry (DPV) were performed in an analytical system, Autolab with PGSTAT 12 (Eco Chemie BV, Utrecht, the Netherlands). The system was run on a PC using GPES and FRA 4.9 software. For impedance measurements, a frequency range of 100 kHz to 0.1 Hz was employed. A conventional three-electrode cell assembly consisting of a platinum wire as an auxiliary electrode and an Ag/AgCl (KCl_{sat}) electrode as a reference electrode was used. The working electrode was either an unmodified carbon nanotubes paste electrode (CNPE) or a carbon nanotubes paste electrode modified with *p*-aminophenol and TiO₂ (*p*-APMCNTPE). The prepared electrodes with carbon nanotubes and with the modifier were characterized by scanning electron microscopy (SEM) (XLC Philips).

Preparation of the modified electrode

p-Aminophenol (50 mg) was dissolved in 10 ml diethyl ether and hand mixed with 840 mg of graphite powder, 550 mg TiO₂ plus 100 mg of multiwall carbon nanotubes in a pestle and mortar. The solvent was evaporated by stirring. Using a syringe, 0.88 g paraffin was added to the mixture and mixed well for 40 min until a uniformly wetted paste was obtained. The paste was then packed into a glass tube. Electrical contact was made by pushing a copper wire down the glass tube into the back of the mixture. When necessary, a new surface was obtained by pushing an excess of the paste out of the tube and polishing it on a weighing paper. The unmodified carbon paste electrode (CPE) was prepared in the same way without adding *p*-aminophenol, TiO₂ and carbon nanotubes to the mixture to be used for comparison purposes.

Preparation of real samples

Five tablets of 6-MP (labelled 50 mg per table (Korea United Pharma, Seoul, S. Korea) were completely ground and homogenized. Then, 100 mg of the powders was accurately weighed and dissolved with ultrasonication in 100 ml of ethanol-water (1 : 1) solution (hot water). The resultant solution was diluted 100 times, and then 1.5 ml of the solution plus 10 ml of 0.10 mol L⁻¹ buffer (pH 9.0) were used for the analysis.

Drug-free human urine used in this study was obtained from healthy volunteers. Urine was also obtained from non-healthy volunteers (from children with cancer – chronic lymphocytic leukaemia). Urine samples were stored in a refrigerator immediately after collection. Ten millilitres of the sample was centrifuged for 5 min at 1500 rpm. The supernatant was diluted five times with universal buffer pH = 9.0. The solution was transferred into the voltammetric cell to be analyzed without any further pretreatment. Standard addition method used for the determination of 6-MP and/or UA in real samples.

Results and discussion

Electrochemistry of the mediator and the electrocatalytic effect

Electrochemical properties of the modified electrode were studied by CV in a buffer solution (pH 9.0). The experimental results showed well-defined and reproducible anodic and cathodic peaks related to *p*-AP/*p*-AP⁺ redox couple with quasi-reversible behaviour and the peak separation potential of ΔE_p ($E_{pa} - E_{pc} = 130 \text{ mV}$).^[44] These cyclic voltammograms were used to examine the variation

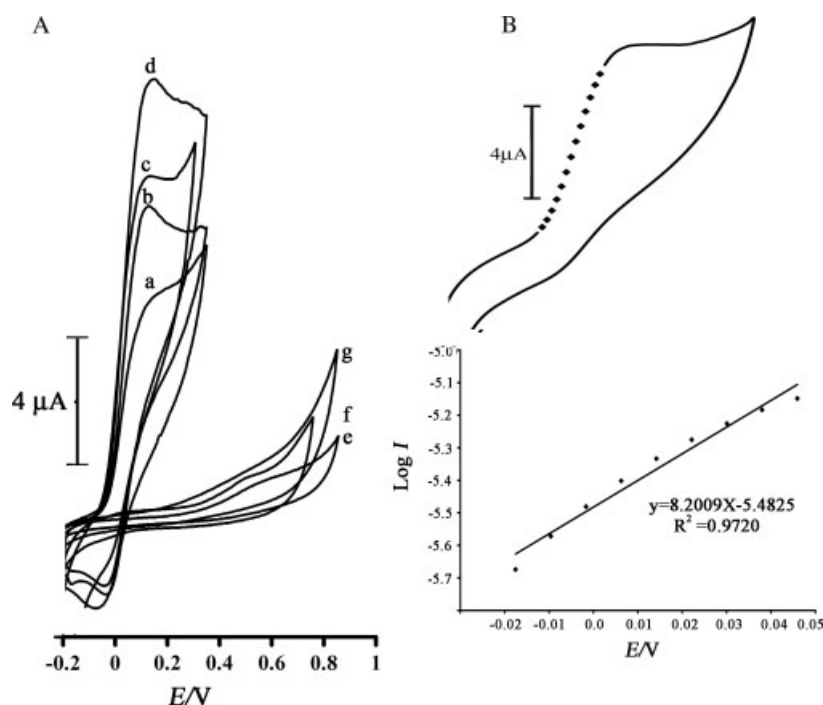


Figure 1. (A) Cyclic voltammograms of a) *p*-APMCNTPE-TiO₂ in the buffer (pH 9.0); b) *p*-APMCPE without TiO₂ in the presence of 400.0 μmol L⁻¹ 6-MP at pH 9.0; c) *p*-APMCNTPE without TiO₂ in the presence of 400.0 μmol L⁻¹ 6-MP at pH 9.0; d) *p*-APMCNTPE-TiO₂ in the presence of 400.0 μmol L⁻¹ 6-MP at pH 9.0; g) as (d), (f) as (c) and (e) as (b) for the unmodified electrode at a scan rate of 10 mV s⁻¹. (B) Tafel plot for *p*-APMCNTPE-TiO₂ the buffer solutions (pH 9.0) with scan rate of 5 mV s⁻¹ in the presence of 300.0 μmol L⁻¹ 6-MP.

of the peak currents vs potential scan rates. The plots of the anodic and cathodic peak currents were linearly dependent on $v^{1/2}$ with a correlation coefficient of 0.9947 and 0.9913 at all the scan rates. This behaviour indicates that the redox process has a diffusion-controlled nature.^[44,45]

Figure 1A depicts cyclic voltammetric responses from the electrochemical oxidation of 400.0 μmol L⁻¹ 6-MP at *p*-APMCNTPE with TiO₂ (curve d), at *p*-aminophenol modified carbon paste (*p*-APMCPE) (curve b), at *p*-APMCNTPE without TiO₂ nanoparticles (curve c), at carbon nanotubes paste electrode (CNTPE) (curve g), at a carbon nanotubes and TiO₂ nanoparticles (curve f) and at a bare carbon paste electrode (CPE) (curve e). As can be seen, the anodic peak potential for the oxidation of 6-MP at *p*-APMCNTPE with and without TiO₂ (curve d and c) and *p*-APMCPE (curve b) is about 110 mV, while it is about 480 mV at CNTPE with TiO₂ (curve g), 500 mV at CNTPE without TiO₂ (curve f), and about 520 mV for 6-MP (curve e) at the bare CPE. From the results, it is concluded that the best electrocatalytic effect for 6-MP oxidation is observed at *p*-APMCNTPE with TiO₂ nanoparticles (curve d). In addition, the results show that the peak potential of 6-MP oxidation at *p*-APMCNTPE (curve d) shifted by about 370, 390, and 410 mV, respectively towards the negative values compared with those at CNTPE (curve g), at CNTPE with TiO₂ (curve f), and at a bare CPE (curve e). Similarly, when we compared the oxidation of 6-MP at *p*-APMCPE (curve b), at *p*-APMCNTPE without TiO₂ (curve c) and at *p*-APMCNTPE with TiO₂ nanoparticles (curve d), an enhancement of the anodic peak current was observed at *p*-APMCNTPE-TiO₂ relative to the value obtained at *p*-APMCPE.

The influence of pH solution on the electro-oxidation of 6-MP at the surface of *p*-APMCNTPE-TiO₂ was studied at different pH values (6.0 to 11.0). The results showed that the maximum electrocatalytic

current was obtained at pH 9.0 and then it's levelled off. In lower pH values, the electro-catalytic effect of *p*-aminophenol decreased due to the protonation of the -NH₂ group. Therefore, pH 9.0 was chosen as the optimum pH for the determination of sulfite at *p*-APMCNTPE-TiO₂.

In order to obtain information on the rate determining step, a Tafel plot was developed for *p*-APMCNTPE-TiO₂ using the data derived from the raising part of the current-voltage curve (Figure 1B). The slope of the Tafel plot is equal to $n(1 - \alpha)F/2.3RT$ which comes up to 8.2009 V decade⁻¹. We obtained $n\alpha$ equal to 0.51. Assuming $n = 1$, then $\alpha = 0.526$.

In addition, the value of αn_{α} (n_{α} is the number of electrons involved in the rate determining step) was calculated for the oxidation of 6-MP at pH 9.0 for both the modified and unmodified carbon nanotubes paste electrodes using the following equation:^[46]

$$\alpha n_{\alpha} = 0.048/(E_p - E_{p/2}) \quad (1)$$

where $E_{p/2}$ is the potential corresponding to $I_{p/2}$. The values for αn_{α} were found to be 0.52 and 0.21 at the surface of both *p*-APMCNTPE and the unmodified carbon nanotubes paste electrode, respectively. These values show that the over-potential of 6-MP oxidation is reduced at the surface of *p*-APMCNTPE, and also that the rate of electron transfer process is greatly enhanced. This phenomenon is thus confirmed by the larger I_{pa} values recorded during cyclic voltammetry at *p*-APMCNTPE. In addition, with increasing the potential scan rate, the catalytic oxidation peak potential gradually shifts towards more positive potentials, suggesting a kinetic limitation in the reaction between the redox site of the *p*-aminophenol and 6-MP. However, the oxidation currents change linearly with the square root of the scan rate, suggesting that at sufficient over-potentials, the reaction

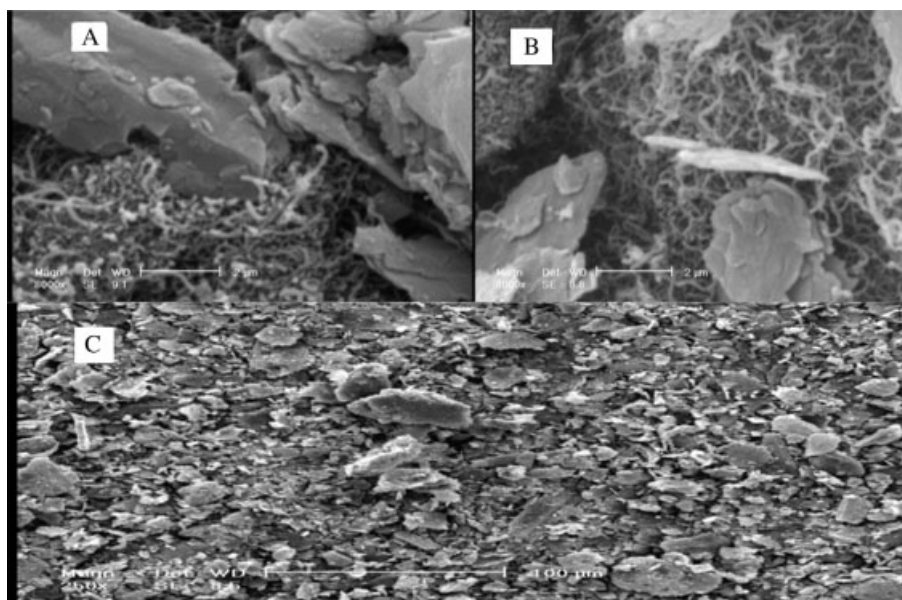


Figure 2. SEM image of (A) *p*-APMCNTPE-TiO₂, (B) Unmodified MCNTPE-TiO₂, and (C) CPE.

is mass transfer controlled. The results show that the overall electrochemical oxidation of 6-MP at the modified electrode might be controlled by the cross-exchange process between 6-MP and the redox site of the *p*-aminophenol and by the diffusion of 6-MP.

SEM characterization of MWCNTs

The morphologies of different electrode surfaces were characterized by SEM. Figure 2 displays a typical morphology of the modified multiwall carbon nanotubes paste electrode with *p*-aminophenol and TiO₂ (Figure 2A), unmodified multiwall carbon nanotubes-TiO₂ paste electrode (Figure 2B), and carbon paste electrode (Figure 2C) characterized by SEM. According to Figures 2A and 2B, most of the MWNTs were in the form of small bundles or single tubes, and the homogeneous dispersion MWNTs could be observed. *p*-Aminophenol and TiO₂ are distributed into MWCNTs and did not change the morphology of MWCNTs, but made it more compact. However, it can be clearly seen that MWCNTs dispersed homogeneously.

Chronoamperometric study

Chronoamperometric behaviour of *p*-APMCNTPE-TiO₂ was examined both in the absence and in the presence of 6-MP by setting the working electrode potential at 0.30 V (in the first potential step) and 0.0 V (in the second potential step) vs Ag|AgCl|KCl_{sat} (Figure 3A). The linearity of the electrocatalytic current vs $t^{-1/2}$ indicates that the current must be controlled by diffusion of 6-MP from the bulk of the solution toward the surface of the electrode (Figure 3B). Therefore, the slope of this linear plot can be used to estimate the diffusion coefficient, *D*, of 6-MP. The mean value of *D* was found to be $2.59 \times 10^{-6} \text{ cm}^2 \text{ s}^{-1}$. These results show that the mediator at the surface of *p*-APMCNTPE-TiO₂ can catalyze the oxidation of 6-MP. It may be concluded that this process corresponds to an EC' mechanism (Diagram 1).

Chronoamperometry can also be employed to evaluate the catalytic rate constant, *k*, for the oxidation reaction of 6-MP at

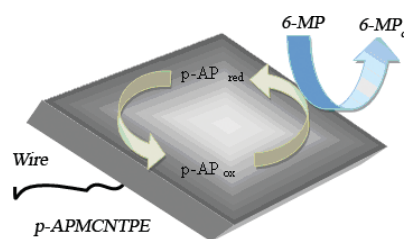


Diagram 1.

p-APMCNTPE-TiO₂ according to the method of Galus:^[47]

$$I_c/I_L = \pi^{1/2} \gamma^{1/2} = \pi^{1/2} (kC_b t)^{1/2} \quad (2)$$

where *I_c* is the catalytic current of 6-MP at *p*-APMCNTPE-TiO₂, *I_L* the limited current in the absence of 6-MP, and $\gamma = kC_b t$ (*C_b* is the bulk concentration of 6-MP) is the argument of the error function and *t* is the time elapsed (s). Based on the slope of *I_c*/*I_L* vs. $t^{1/2}$ plot, *k* can be obtained for a given 6-MP concentration. The plots obtained from the chronoamperograms in Figure 3 are presented in Figure 3C. From the values of the slopes, an average value obtained as $91.71 \times 10^3 \text{ mol}^{-1} \text{ L s}^{-1}$.

Electrochemical impedance spectroscopy

Figure 4A presents Nyquist diagrams and bode plots of the imaginary impedance (*Z_{im}*) vs the real impedance (*Z_{re}*) of the electrochemical impedance spectroscopy (EIS) obtained at *p*-APMCNTPE-TiO₂ recorded at 0.150 V dc-offset in the absence (curve a) and in the presence of $1000 \mu\text{mol L}^{-1}$ UA (curve b) and $1000 \mu\text{mol L}^{-1}$ 6-MP (curve c), respectively. Figure 4A shows that in the absence of 6-MP, the Nyquist diagram comprises a depressed semicircle at high frequencies which may be related to the combination of the double-layer capacitance and charge transfer resistance of *p*-aminophenol electro-oxidation, followed by a straight line with a slope of nearly 45° that is due to the occurrence of mass transport process via diffusion.

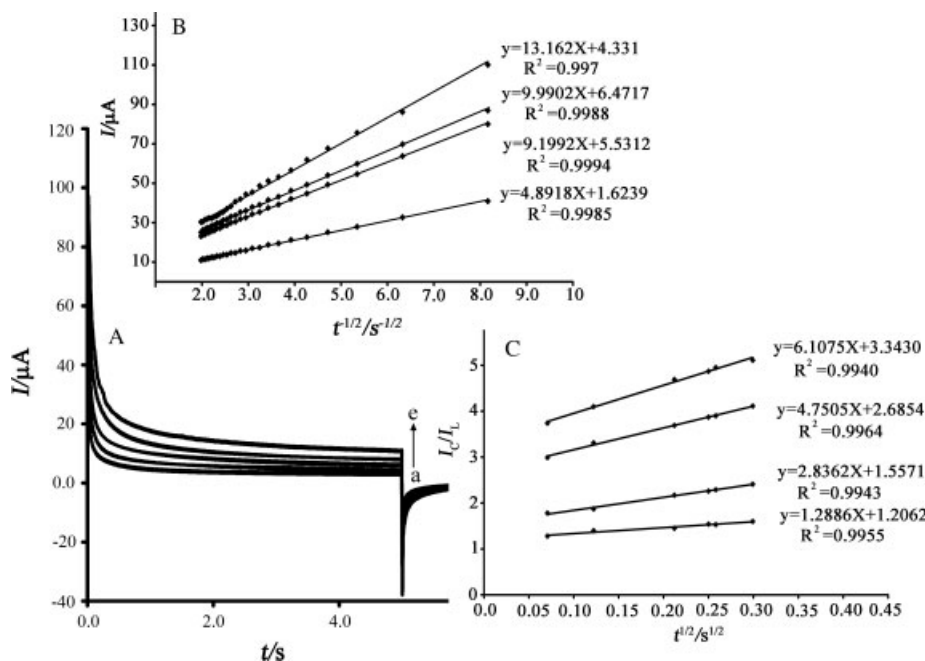


Figure 3. (A) Chronoamperograms obtained at the *p*-APMCNTPE-TiO₂ in the absence a) and presence of b) 250, c) 350, d) 500 and e) 600 $\mu\text{mol L}^{-1}$ 6-MP (pH 9.0). (B) Cottrell's plot for data of the chronoamperograms. (C) Dependence of I_c/I_L on the $t^{1/2}$ derived from the chronoamperogram data.

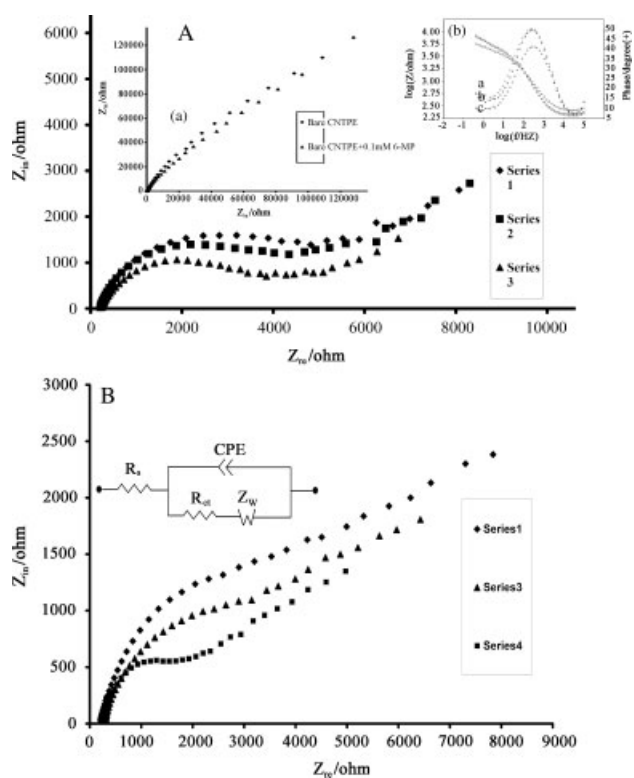


Figure 4. (A) Nyquist diagrams of *p*-APMCNTPE-TiO₂ in the absence (a) and presence of 1000 $\mu\text{mol L}^{-1}$ UA (b), and 1000 $\mu\text{mol L}^{-1}$ 6-MP (c). Inset (a) shows Nyquist diagrams for 6-MP at CNTPE. Points show the experimental data and the full line is calculated from the optimized parameters. Inset (b) shows the related bode plots of (a), (b) and (c). (B) Complex plane plots obtained on the modified electrode for different concentrations of 6-MP as: a) 1000, b) 1300, and c) 1500 $\mu\text{mol L}^{-1}$. Conditions: pH, 9.0; E_{DC} , +0.15 V vs. Ag/AgCl; E_{AC} , 5 mV; Frequency range, 10 kHz to 1 Hz. Inset shows equivalent circuit compatible with the Nyquist diagram.

The equivalent circuit compatible with the Nyquist diagram recorded in the absence and presence of 6-MP is depicted in Figure 4B (insert). In this circuit, R_s , CPE, and R_{ct} represent solution resistance, a constant phase element corresponding to the double-layer capacitance, and the charge transfer resistance associated with the oxidation of low-valence *p*-aminophenol species. W is a finite-length Warburg short-circuit term coupled to R_{ct} , which accounts for the Nernstian diffusion. In the presence of 6-MP, the diameter of the semicircle decreases, confirming the electrocatalytic capability of the mentioned electrocatalyst for 6-MP oxidation. This is due to the instant chemical reaction of 6-MP with the high-valence *p*-aminophenol species. The catalytic reaction of oxidation of 6-MP that occurred via the participation of *p*-aminophenol species virtually caused an increase in the surface concentration of low valence species of the electrocatalyst, and the charge transfer resistance declined, depending on the concentration of 6-MP in the solution. On the other hand, UA could not be electrocatalyzed on this modified electrode to provide the necessary conditions for the selective determination of 6-MP in real samples. This behaviour is consistent with the result of the CV and chronoamperometry (Figures 1 and 2). In the abovementioned circuits, the charge-transfer resistance of the electrode reaction is the only circuit element that has a simple physical meaning describing how fast the rate of charge transfer during electro-oxidation of 6-MP changes with the electrode potential. To obtain a satisfactory fitting of Nyquist diagrams, it was necessary to replace the double-layer capacitance with a constant phase element in the equivalent circuit. The dependence of the drug concentration on R_{ct} has been illustrated in Figure 3B. It is interesting that the concentration of 6-MP is related to R_{ct} of Nyquist diagrams. The equation $R_{ct} = RT \times (n^2 F^2 A k_{ct} [S])^{-1}$ may explain the relation between bulk concentration of the redox probe and charge transfer resistance, where R is the ideal gas constant, T is the absolute temperature, n is the number of transferred electrons per one molecule of the redox probe, F is Faraday's constant, A is the

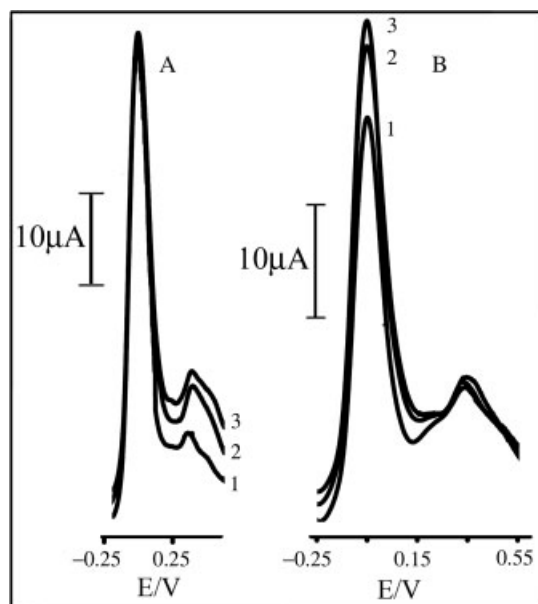


Figure 5. DP voltammograms of 6-MP and UA under the optimum conditions. (A) $3.3 \mu\text{mol L}^{-1}$ 6-MP with UA concentrations of 1): 18.0; 2): 120.0; and 3): $140.0 \mu\text{mol L}^{-1}$; (B) $150.0 \mu\text{mol L}^{-1}$ UA with 6-MP concentrations of 1): 1.2; 2): 3.0; and 3): $3.6 \mu\text{mol L}^{-1}$.

geometric surface area of the electrode (cm^2), k_{ct} is the potential dependent charge transfer rate constant, and $[S]$ corresponds to the concentration of the redox probe (mol cm^{-3}). We can replace $[S]$ with $k_1[6\text{-MP}]$, where k_1 is a constant. If all the other parameters are also constant, simply a linear relation of the form $1/R_{\text{ct}} = k[6\text{-MP}]$ is obtained, in which k includes all constants. As a result, the values of the charge transfer resistances gradually decrease upon addition of 6-MP to the solution. The extent of the decrease in R_{ct} depends on the magnitude of the applied DC potential, provided the AC potential is small and the diffusion layer produced by the DC potential is not perturbed by the AC potential.

Figures of merit

Since DPV has a much higher current sensitivity and better resolution than CV, DPV was used for simultaneous determination of 6-MP and UA. The pulse height and width of 50 mV and 5 mV were selected in order to get the best sensitivity under the specific conditions. The results showed two linear segments with different slopes for 6-MP concentration; namely, for $0.09\text{--}4.5 \mu\text{mol L}^{-1}$ of 6-MP, the regression equation was $I_p(\mu\text{A}) = (6.0828 \pm 0.0701)C_{6\text{-MP}} + (44.0490 \pm 0.8000)$ ($r^2 = 0.9968$, $n = 6$), while for $4.5\text{--}350 \mu\text{mol L}^{-1}$ of 6-MP, the regression equation was $I_p(\mu\text{A}) = (0.0968 \pm 0.0011)C_{6\text{-MP}} + (71.1250 \pm 1.0101)$ ($r^2 = 0.9937$, $n = 7$), where $C_{6\text{-MP}}$ is $\mu\text{mol L}^{-1}$ concentration of 6-MP.

The detection limit was determined at $0.065 \mu\text{mol L}^{-1}$ 6-MP according to the definition of $Y_{\text{LOD}} = Y_B + 3\sigma$.^[48]

In addition, analytical experiments were carried out either by varying UA concentration ($18\text{--}150 \mu\text{mol L}^{-1}$) in the presence of fixed amounts of 6-MP ($3.3 \mu\text{mol L}^{-1}$) and/or varying 6-MP concentration ($0.6\text{--}2.0 \mu\text{mol L}^{-1}$) in the presence of fixed amounts of UA ($50 \mu\text{mol L}^{-1}$) (Figures 4A and 4B). The results showed no intermolecular interactions during the oxidation of the compounds at the surface of the electrode. The DP voltammetric results showed that simultaneous determination of 6-MP and UA with two well-distinguished anodic peaks at

-30 and 350 mV potentials, corresponding to the oxidation of 6-MP and UA, is possible at the modified electrode. Fig. 5 shows DP voltammograms of different concentrations of 6-MP and UA under the optimum conditions.

The sensitivities towards 6-MP in the absence and presence of UA were found to be $6.0828 \pm 0.0701 \mu\text{A } \mu\text{mol L}^{-1}$ (in the absence of UA) and $6.1669 \pm 0.1030 \mu\text{A } \mu\text{mol L}^{-1}$ (in the presence of UA). It is interesting to note that the sensitivities of the modified electrode to 6-MP in the absence and presence of UA are virtually close, which indicates that the oxidation processes of 6-MP and UA at $p\text{-APMCNTPE-TiO}_2$ are independent.

The repeatability and stability of $p\text{-APMCNTPE-TiO}_2$ was investigated by CV measurements of 1.0 and $15.0 \mu\text{mol L}^{-1}$. The relative standard deviation (RSD%) for ten successive assays were 0.7% and 1.2%, respectively. When using five different electrodes, the RSD% for five measurements was 3.5%. When stored in a laboratory, $p\text{-APMCNTPE-TiO}_2$ retains 94% of its initial response after a week and 90% after 20 days. These results indicate that $p\text{-APMCNTPE-TiO}_2$ has good stability and reproducibility, and could be used for 6-MP measurements.

Interference study

The influence of various substances as compounds potentially interfering with the determination of 6-MP and UA were studied with $3.0 \mu\text{mol L}^{-1}$ 6-MP and $100.0 \mu\text{mol L}^{-1}$ UA. The potentially interfering substances were chosen from the group of substances commonly found with 6-MP and UA in pharmaceuticals and/or in biological fluids. The tolerance limit was defined as the maximum concentration of the interfering substance that caused an error of less than $\pm 5\%$ for the determination of 6-MP and UA. We found that neither 1000-fold of glucose, sucrose, lactose, fructose, and citric acid nor 600-fold of methanol, ethanol, Ca^{2+} , Mg^{2+} , SO_4^{2-} , Al^{3+} , NH_4^+ , Fe^{2+} , Fe^{3+} , CO_3^{2-} , Cl^- , F^- , glycine, citric acid, aspartic acid, and nor 600-fold of aspirin affected selectivity. Nor did saturation of starch solution, 50-fold of urea, and 5-fold dopamine, ascorbic acid and epinephrine interfere with the determination of 6-MP and UA. Although ascorbic acid show interference, but interference from ascorbic acid can be minimized by using ascorbic oxidase enzyme, which exhibits high selectivity to oxidation of ascorbic acid, if necessary.

Sample analysis

To evaluate the applicability of the proposed method, the recovery of 6-MP was determined for 6-mercaptopurine in urine and tablet samples. Drug-free human urine used in this study was obtained from healthy volunteers. Urine was also obtained from children who have cancer (chronic lymphocytic leukaemia). The results are given in Table 2. In addition, the results for urine sample were compared with an HPLC method^[18] with satisfactory results.

Conclusions

In this paper, we studied the electrochemical behaviour of 6-MP and UA at $p\text{-APMCNTPE-TiO}_2$ using voltammetric methods. The results showed that the oxidation of 6-MP is catalyzed at pH 9.0 and that the peak potential of 6-MP is shifted by 370 mV to a less positive potential at the surface of $p\text{-APMCNTPE-TiO}_2$. The modified electrode exhibits highly electrocatalytic activity for the oxidation

Table 2. Determination of 6-MP and UA in real samples ($n = 5$)

Sample	6-MP Added ($\mu\text{mol L}^{-1}$)	UA Added ($\mu\text{mol L}^{-1}$)	6-MP			UA			HPLC standard method ($\mu\text{mol L}^{-1}$)
			Found ($\mu\text{mol L}^{-1}$)	Recovery (%)	RSD (%)	Found ($\mu\text{mol L}^{-1}$)	Recovery (%)	RSD (%)	
Urine ^a	–	<LOD*	–	–	–	<LOD	–	–	<LOD
	10.0	–	9.7	97.0	3.1	10.5	105.0	2.8	–
	20.0	20.0	20.2	101.0	2.7	21.0	105.0	1.1	–
	30.0	30.0	30.3	101.0	2.2	30.5	101.6	0.9	–
Urine ^b	–	–	3.0	–	3.2	–	–	–	2.9
	5.0	–	8.1	102.0	2.6	–	–	–	–
Urine ^c	–	–	0.2	–	2.4	–	–	1.9	0.24
	2.0	–	2.2	102.0	2.5	–	–	2.2	–
Urine ^d	–	–	0.5	–	1.9	–	–	–	0.51
	4.5	–	5.1	102.0	2.4	–	–	–	–
Urine ^e	–	–	0.4	–	2.2	–	–	–	0.42
	1.6	–	2.1	105.0	2.7	–	–	–	–
Tablet ^f	–	–	9.6	96.0	1.5	–	–	–	–
	5.0	–	15.1	100.6	2.1	–	–	–	–
	10.0	–	20.2	101.0	1.8	–	–	–	–

* LOD: Limit of detection.

^a Healthy person. ^b Sampling was made after 2.5 h from a man who is safe and used 6-MP.^{c,d} and ^e Urine samples of patients undergoing treatment with 6-MP.^f Expected value = $10 \mu\text{mol L}^{-1}$.

of 6-MP and UA. Although the oxidation peak of UA overlapped with that of 6-MP with the other electrodes, this electrode was able to differentiate the substances and it is, therefore, possible to measure both simultaneously. Furthermore, the proposed modified electrode displayed higher selectivity in voltammetric measurements of 6-MP and UA in their mixture solution.

Acknowledgement

The authors wish to thank Isfahan University of Technology (IUT) Research Council and the Center of Excellence for Sensor Technology (IUT) for their support.

References

- S. Sahasranaman, D. Howard, S. Roy. Clinical pharmacology and pharmacogenetics of thiopurines. *Eur. J. Clin. Pharmacol.* **2008**, *64*, 753.
- T. Dervieux, R. Boulieu. A HPLC method for the monitoring of human red cell 6-thioguanine and methyl 6-mercaptopurine nucleotides in a single run. *Clin. Biochem.* **1997**, *30*, 248.
- H. J. Breter, H. Mertes. The quantitative determination of metabolites of 6-mercaptopurine in biological materials. VII. Chemical synthesis by phosphorylation of 6-thioguanosine 5'-monophosphate, 5'-diphosphate and 5'-triphosphate, and their purification and identification by reversed-phase/ion-pair high-performance liquid chromatography and by various enzymatic assays. *Biochim. Biophys. Acta* **1990**, *1033*, 124.
- L. E. Lavi, J. S. Holcenberg. A rapid and sensitive high-performance liquid chromatographic assay for 6-mercaptopurine metabolites in red blood cells. *Anal. Biochem.* **1985**, *144*, 514.
- R. Boulieu, T. Dervieux. High-performance liquid chromatographic determination of methyl 6-mercaptopurine nucleotides (Me6-MPN) in red blood cells: analysis of Me6-MPN per se or Me6-MPN derivative? *J. Chromatogr. B* **1999**, *730*, 273.
- A. F. Hawwa, J. S. Millership, P. S. Collier, J. C. McElroy. Development and validation of an HPLC method for the rapid and simultaneous determination of 6-mercaptopurine and four of its metabolites in plasma and red blood cells. *J. Pharm. Biomed. Anal.* **2009**, *49*, 401.
- M. Ng, T. F. Blaschke. Analysis of free intracellular nucleotides using high-performance capillary electrophoresis. *Anal. Chem.* **1992**, *64*, 1682.
- T. Tsuda, G. Nakagawa, M. Sato, K. Yagi. Separation of nucleotides by high-voltage capillary electrophoresis. *J. Appl. Biochem.* **1983**, *5*, 330.
- S. Georget, J. Vigneron, I. May, A. Perrin, M. A. Hoffman, M. Hoffman. Determination by capillary zone electrophoresis of mercaptopurine and thioguanine concentration in capsules for paediatric patients. *J. Clin. Pharm. Ther.* **2003**, *24*, 273.
- C. C. Wang, S. S. Chiou, S. M. Wu. Determination of mercaptopurine and its four metabolites by large-volume sample stacking with polarity switching in capillary electrophoresis. *Electrophoresis* **2005**, *26*, 2639.
- B. Y. Lu, H. Li, H. Deng, Z. Xu, W. S. Li, H. Y. Chen. Voltammetric determination of 6-mercaptopurine using [Co(phen)3]³⁺/MWNT modified graphite electrode. *J. Electroanal. Chem.* **2008**, *621*, 97.
- M. G. Li, Y. L. Wang, G. F. Wang, B. Fang. Electrochemical determination of 6-mercaptopurine at silver microdisk electrodes. *Anal. di Chem.* **2005**, *95*, 685.
- L. Wang, Z. Zhang. The study of oxidization fluorescence sensor with molecular imprinting polymer and its application for 6-mercaptopurine (6-MP) determination. *Talanta* **2008**, *76*, 768.
- X. C. Shen, L. F. Jiang, H. Liang, X. Lu, L. J. Zhang, X. Y. Liu. Determination of 6-mercaptopurine based on the fluorescence enhancement of Au nanoparticles. *Talanta* **2006**, *69*, 456.
- A. Besada, N. B. Tadros, Y. A. Gawargious. Copper(II)-neocuproine as colour reagent for some biologically active thiols: Spectrophotometric determination of cysteine, penicillamine, glutathione, and 6-mercaptopurine. *Microchim. Acta* **1989**, *99*, 143.
- S. R. Rabel, J. F. Stobaugh, R. Truworthy. Determination of intracellular levels of 6-mercaptopurine metabolites in erythrocytes utilizing capillary electrophoresis with laser-induced fluorescence detection. *Anal. Biochem.* **1995**, *224*, 315.
- X. N. Cao, L. Lin, Y. Y. Zhou, G. Y. Shi, W. Zhang, K. Yamamoto, L. T. Jin. Amperometric determination of 6-mercaptopurine on functionalized multi-wall carbon nanotubes modified electrode by liquid chromatography coupled with microdialysis and its application to pharmacokinetics in rabbit. *Talanta* **2003**, *60*, 1063.
- X. N. Cao, L. Lin, Y. Y. Zhou, W. Zhang, G. Y. Shi, K. Yamamoto, et al. Study of the interaction of 6-mercaptopurine with protein by microdialysis coupled with LC and electrochemical detection based on functionalized multi-wall carbon nanotubes modified electrode. *J. Pharm. Biomed. Anal.* **2003**, *32*, 505.

- [19] L. Lin, P. H. Qiu, X. F. Xie, X. N. Cao, L. T. Jin. Determination of 6-mercaptopurine in rat blood by microdialysis coupled with high performance liquid chromatography on a functionalized multiwall carbon nanotube-modified electrode. *Chem. Res. Chin. Univ.* **2005**, *21*, 141.
- [20] X. C. Shen, L. F. Jiang, H. Liang, X. Lu, L. J. Zhang, X. Y. Liu. Determination of 6-mercaptopurine based on the fluorescence enhancement of Au nanoparticles. *Talanta* **2006**, *69*, 456.
- [21] A. J. Viudez, R. Madueno, T. Pineda, M. Blazquez. Stabilization of gold nanoparticles by 6-mercaptopurine monolayers. Effects of the solvent properties. *J. Phys. Chem. B* **2006**, *110*, 17840.
- [22] P. Podsiadlo, V. A. Sinani, J. H. Bahng, N. W. S. Kam, J. Lee, N. A. Kotov. Gold nanoparticles enhance the anti-leukemia action of a 6-mercaptopurine chemotherapeutic agent. *Langmuir* **2008**, *24*, 568.
- [23] S. Shahrokhian, H. R. Zare-Mehrjardi. Simultaneous voltammetric determination of uric acid and ascorbic acid using a carbon-paste electrode modified with multi-walled carbon nanotubes/nafion and cobalt(II)nitrosalophen. *Electroanalysis* **2007**, *19*, 2234.
- [24] M. Mazloum Ardakani, Z. Akrami, H. Kazemian, H. R. Zare. Electrocatalytic characteristics of uric acid oxidation at graphite-zeolite-modified electrode doped with iron (III). *J. Electroanal. Chem.* **2006**, *586*, 31.
- [25] M. A. T. Gilmartin, J. P. Hart. Voltammetric and amperometric behavior of uric acid at bare and surface-modified screen-printed electrodes: studies towards a disposable uric acid sensor. *Analyst* **1992**, *117*, 1299.
- [26] T. Tatsuma, T. Watanabe. Oxidase/peroxidase bilayer-modified electrodes as sensors for lactate, pyruvate, cholesterol and uric acid. *Anal. Chim. Acta* **1991**, *242*, 85.
- [27] F. F. Zhang, X. L. Wang, C. X. Li, X. H. Li, Q. Wan, Y. Z. Xian, *et al.* Assay for uric acid level in rat striatum by a reagentless biosensor based on functionalized multi-wall carbon nanotubes with tin oxide. *Anal. Bioanal. Chem.* **2005**, *382*, 1368.
- [28] S. Shahrzad, T. Ghazian. *Iran Pharmacology*, Tehran University Publication: Tehran, Iran, **2002**.
- [29] Q. Zhao, Z. Gan, Q. Zhuang. Electrochemical sensors based on carbon nanotubes. *Electroanalysis* **2002**, *14*, 1609.
- [30] A. Merkoci. Carbon nanotubes in analytical sciences. *Microchim. Acta* **2006**, *152*, 157.
- [31] A. Merkoci, M. Pumera, X. Llopis, B. Pérez, M. Del Valle, S. Alegret. New materials for electrochemical sensing VI: Carbon nanotubes. *Trends Anal. Chem.* **2005**, *24*, 826.
- [32] J. J. Gooding. Nanostructuring electrodes with carbon nanotubes: A review on electrochemistry and applications for sensing. *Electrochim. Acta* **2005**, *50*, 3049.
- [33] A. Merkoci. Nanobiomaterials in electroanalysis. *Electroanalysis* **2007**, *19*, 739.
- [34] J. Wang. Carbon-nanotube based electrochemical biosensors: a review. *Electroanalysis* **2005**, *17*, 7.
- [35] M. Trojanowicz. Analytical applications of carbon nanotubes: a review. *Trends Anal. Chem.* **2006**, *25*, 480.
- [36] A. A. Ensafi, H. Karimi-Maleh. Modified multiwall carbon nanotubes paste electrode as a sensor for simultaneous determination of 6-thioguanine and folic acid using ferrocenedicarboxylic acid as a mediator. *J. Electroanal. Chem.* **2010**, *640*, 75.
- [37] P. M. Ajayan. Nanotubes from carbon. *Chem. Rev.* **1999**, *99*, 1787.
- [38] T.W.Odom, J. L. Huang, P. Kim, C. M. Lieber. Atomic structure and electronic properties of single-walled carbon nanotubes. *Nature* **1998**, *391*, 62.
- [39] H. Yaghoobian, H. Karimi-Maleh, M. A. Khalilzadeh, F. Karimi. Electrocatalytic oxidation of levodopa at a ferrocene modified carbon nanotube paste electrode. *Int. J. Electrochem. Sci.* **2009**, *4*, 993.
- [40] G. Zhao, Z. Yin, L. Zhang, X. Xian. Direct electrochemistry of cytochrome c on a multi-walled carbon nanotubes modified electrode and its electrocatalytic activity for the reduction of H₂O₂. *Electrochem. Commun.* **2005**, *7*, 256.
- [41] S. Wei, F. Zhao, B. Zeng. Electrochemical behavior and determination of uric acid at single-walled carbon nanotube modified gold electrodes. *Microchim. Acta* **2005**, *150*, 219.
- [42] H. Beitollahi, H. Karimi-Maleh, H. Khabazzadeh. Nanomolar and selective determination of epinephrine in the presence of norepinephrine using carbon paste electrode modified with carbon nanotubes and novel 2-(4-oxo-3-phenyl-3,4-dihydro-quinazolinyl)-N'-phenyl-hydrazinecarbothioamide. *Anal. Chem.* **2008**, *80*, 9848.
- [43] A. A. Ensafi, M. Taei, T. Khayamian, H. Karimi-Maleh, F. Hasanpour. Voltammetric measurement of trace amount of glutathione using multiwall carbon nanotubes as a sensor and chlorpromazine as a mediator. *J. Solid State Electrochem.* **2010**, *14*, 1415.
- [44] E. Mirmomtaz, A. A. Ensafi, H. Karimi-Maleh. Electrocatalytic determination of 6-thioguanine at a p-aminophenol modified carbon paste electrode. *Electroanalysis* **2008**, *20*, 1973.
- [45] A. A. Ensafi, E. Khoddami, B. Rezaei, H. Karimi-Maleh. p-Aminophenol-multiwall carbon nanotubes-TiO₂ electrode as a sensor for simultaneous determination of penicillamine and uric acid. *Coll. Surf. B Biointerfaces* **2010**, *81*, 42.
- [46] M. H. Pournaghi-Azar, H. Razmi-Nerbin. Electrocatalytic characteristics of ascorbic acid oxidation at nickel plated aluminum electrodes modified with nickel pentacyanonitrosylferrate films. *J. Electroanal. Chem.* **2000**, *488*, 17.
- [47] Z. Galus. *Fundamentals of Electrochemical Analysis*, Ellis Horwood: New York, **1976**.
- [48] J. N. Miller, J. C. Miller. *Statistics and Chemometrics for Analytical Chemistry*, 4th ed., Pearson Education Ltd: Essex, England, **2000**.